# Improved Block Based Feature Level Image Fusion Technique using Multiwavelet with Neural Network

### C. M. Sheela Rani, V. VijayaKumar, B. V. Ramana Reddy

*Abstract— Image fusion is defined as the process of combining two or more different images into a new single image retaining the important features from each image with extended information content. To overcome the spectral distortions in the fused image, many multiresolution based approaches have been proposed. They include different pyramid transforms and discrete scalar wavelet transforms. The multiwavelet transform (MWT) produces a non-redundant image representation, which provides better spatial and spectral localization of image formation. This paper has derived an efficient block based feature level multiwavelet transform with neural network (BFMN) model for image fusion. The proposed (BFMN) model integrates MWT with neural network, which is one of the feature extraction or detection machine learning applications. In the proposed BFMN model, the two fusion techniques, multiwavelet transform (MWT) and neural network (NN) are discussed for fusing the IRS-1D images using LISS III scanner about the locations Hyderabad, Vishakhapatnam, Mahaboobnagar and Patancheru in Andhra Pradesh, India. Also QuickBird image data and Landsat 7 image data are used to perform experiments on the proposed BFMN model. The features under study are contrast visibility, spatial frequency, energy of gradient, variance and edge information. Feed forward back propagation neural network is trained and tested for classification since the learning capability of neural network makes it feasible to customize the image fusion process. The trained neural network is then used to fuse the pair of source images. The proposed BFMN model is compared with other techniques to assess the quality of the fused image. Experimental results clearly prove that the proposed BFMN model is an efficient and feasible algorithm for image fusion.*

*Index Terms— Image Fusion, Multiwavelet Transform, GHM multiwavelet, Mutual information, Performance Analysis.*

## I. INTRODUCTION

In the area of satellite imagery, the purpose of image fusion is to merge the gray-level high-resolution panchromatic image (PAN) with the coloured low-resolution multispectral image (MS) to produce an image which contains the best information coming from the original images. The source images are assumed to be "perfectly" registered since they are obtained from different sensors having different resolutions.

In remote sensing fields, a MS image contains colour information that is produced by three sensors covering the red, green and blue spectral wavelengths and a PAN image has a high number of pixels (high spatial resolution) but without color information. Since MS image has poor spatial resolution, there is a need to fuse it with PAN image to obtain a fused image which contains the geometric details of the

PAN image and the colour information of the MS image. Hence, the fused image is a high-resolution MS image.

The fused image should have few following requirements - it should preserve all relevant information contained in the input images and it should not introduce any artefacts or inconsistencies. A straightforward approach is to compute the average of all the pixel values to generate a fused image. Even though this approach is simple, the low contrast of the fused image seriously limits its usage. To overcome this limitation, multiresolution based approaches were proposed. K. Kannan et al. evaluated the performance of all the levels of multi-focused images using different wavelet transforms [1]. Dong et al. discussed clearly various advances in multi-sensor data fusion [2].

Image fusion using MWT produces the fused image with more defined features because of its ability to merge images in multiwavelet space with different frequencies processed differently. The objective of image fusion schemes is to extract all the useful information from the source images. MWT offers simultaneous orthogonality, symmetry, compact support, and vanishing moment, which are not possible with wavelet transform. Nava et al. presented a technique to construct a multiscale representation of planar contours based on multiwavelet transform. Liang et al. proposed an embedded image coding scheme using the multiwavelet transform and inter-subband prediction [3]. B.Martin and E.Bell presented new multiwavelet transform and quantization methods and introduced multiwavelet packets [4]. Nava et al. presented a multiscale representation of planar contours based on the multiwavelet transform [5].

Image fusion techniques range from the simplest method of pixel averaging to more sophisticated methods such as integrating multi-resolution transform with neural networks and so on. The proposed BFMN model integrates MWT with neural network, which is one of the feature extraction and detection machine learning applications to take a decision. Siddiqui et al. proposed an algorithm for block-based feature-level multi-focus image fusion in [6]. G. Piella proposed a region-based multi-resolution image fusion algorithm which combines the aspects of region and pixel-based fusion [7]. Riazifar et al. proposed a compression scheme in transform domain and compared the performance of both discrete wavelet transform and contourlet transform [8]. Khosravi. et al. proposed a block feature based image fusion algorithm which integrates multiwavelet transform with the feed forward probabilistic neural networks for the images which are in and out of focus [9].

Artificial Neural Networks (ANNs) proved to be a more powerful and self-adaptive method of pattern recognition as compared to traditional linear and simple nonlinear analysis [10], [11].

**C. M. Sheela Rani**, Research Scholar, Dept of Computer Science & Engg, Acharya Nagarjuna University, Guntur, India.
**V. VijayaKumar**, Dept of Computers, Head SSRF, GIET, JNTUK, Rajahmundry, A.P, India.
**B. V. Ramana Reddy**, Assoc. Prof in CSE, JNTUH, Hyderabad, Andhra Pradesh, India

Li et al. describes the application of *artificial* neural networks to pixel-level fusion of multi-focus images taken from the same scene [12]. Sahoolizadeh et al. proposed a new hybrid approach for face recognition using Gabor Wavelets and Neural Networks [13]. Rong *et al.* presented a feature-level image fusion method based on segmentation region and neural networks. David et al. presented a block feature based image fusion for the images which are in focus and out of focus using MWT [14]. Khosravi et al. proposed a block feature based image fusion for the images which are in focus and out of focus using Multiwavelet transforms [15]. The results indicated that this combined fusion scheme is more efficient than that of traditional methods [16].

The first step of ANN-based data fusion is to fuse the two registered images and decompose into several blocks with some defined size. Then, the features from the two images of the corresponding blocks are extracted and the normalized feature vector incident to neural network can be constructed [15]. The features generally used are spatial frequency, visibility, edge, etc. The next step is to select some vector samples to train neural networks. After training, the ANN model can remember a functional relationship and be used for further calculations. For these reasons, the ANN concept has been adopted to develop strongly nonlinear models for multiple sensors of data fusion.

The rest of this paper is organized as follows. Section 2 describes about image fusion based on MWT. Section 3 describes about feature extraction and the proposed BFMN algorithm. In section 4, quality assessment techniques are discussed. Section 5 presents some experimental results and comparisons. Finally, this paper is concluded in section 6.

## II. IMAGE FUSION BASED ON MULTIWAVELET TRANSFORM

The standard fusion methods such as averaging, principle component analysis, intensity hue saturation, etc., perform well spatially but usually introduce some spectral distortions. To overcome this problem, numerous multiscale transform based fusion schemes have been proposed. The multiresolution transforms include pyramid transforms such as the laplacian pyramid, gradient pyramid, ratio of lowpass pyramid, and discrete wavelet transform [17]. The most commonly used transform for image fusion at multi-scale is wavelet transform, since it minimizes structural distortions. For best performance, wavelet transforms require filters that combine a number of desirable properties, such as orthogonality, symmetry and higher order of approximation. Discrete wavelet transform suffers from lack of shift invariance & poor directionality which can be handled by using multiwavelets. Multiwavelets are extensions of discrete wavelets. Discrete wavelet transform are also called as scalar wavelets. Multiwavelets are almost similar to scalar wavelets but have few important differences. Multiwavelets have two or more scaling functions and two or more mother wavelet functions used for signal representation. In the research area of wavelet transforms, design and analysis of multiwavelets is a new development. Hence, multiwavelets should perform better than wavelets due to the flexibility provided in the design of multi-filters.

The MWT filters are given by GHM (Geronimo-Hardin-Massopust), CL (Chu-Lian), and SA (Shen-Tan-Tham). Among these filters, GHM filter is famous which is proposed by [18] [19]. The GHM basis offers a combination of orthogonality, symmetry, and compact support which cannot be achieved by any scalar wavelets except for Haar wavelet [20]. Few methods were proposed for the construction of orthogonal and biorthogonal multifilters with some desirable filter properties [21], [22]; good pre-processing techniques [23], [24]. Goodman and Lee are the first researchers to develop a multiresolution theory of multiwavelets [25].

In particular, scalar wavelets have a single scaling function $\phi(t)$ and wavelet function $\Psi(t)$ where as multiwavelets have two or more scaling functions and two or more wavelet functions. The set of scaling functions can be denoted by using the vector notation, $\phi(t) \equiv \left[\phi_1(t)\ \phi_2(t) \dots \dots \phi_r(t)\right]^T$ where $\phi(t)$ is called the multiscaling function. Likewise, the multiwavelet function is defined from the set of wavelet functions as $\Psi(t) \equiv \left[\Psi_1(t)\ \Psi_2(t) \dots \dots \Psi_r(t)\right]^T$ where $\Psi(t)$ is called the multiwavelet function. When r=1, $\Psi(t)$ is a scalar wavelet.

Each decomposition level of multiwavelets consists of 16 subbands. For instance, the lowpass subband consists of four blocks as illustrated in Figure 1. These local subbands are characterized by different spectral properties and make $i^{th}$ level decomposition using discrete multiwavelets look like $(i+1)^{th}$ level decomposition using discrete scalar wavelets [10]. The detail subbands (horizontal, vertical, and diagonal) consist of blocks having similar spectral content. Except for the lowpass subband, all other subbands contain transform values that fluctuate around zero [11]. While the lowpass subband is an approximation of the input image and the three detail subbands convey information about the detail parts in horizontal, vertical and diagonal directions. Different merging procedures can be applied to approximation and detail subbands. Lowpass subbands will be merged using simple averaging operations since they both contain approximations of the source images. A selection procedure is applied to the multiwavelet coefficients of the three detail subbands.

| LOLO | L1 LO | LO HO | L1 HO |
|------|-------|-------|-------|
| LO L1 | L1 L1 | LO H1 | L1 H1 |
| HO LO | H1 LO | HO HO | HO H1 |
| HO L1 | HO LO | HO H1 | H1 H1 |

**Figure 1. The decomposition level consists of 16 subbands**
**Let a scaling function $\Phi(t)$ generates a multi resolution analysis as defined in equation (1).**

$$\varphi(t) = \sum_k C_k \varphi(2t - k) \qquad (1)$$

where $C_k$ is the coefficients associated with these scaling functions. There are 'r' wavelets $W_0(t), \dots W_{r-1}(t)$ satisfying the matrix wavelet equation as defined in equation (2)

$$W(t) = \sum_k D_k \varphi(2t - k) \qquad (2)$$

To implement MWT, new filter bank structures are used where the lowpass and highpass filter banks are matrices rather than the scalars i.e.,

the two scaling and two wavelet functions satisfy the following two-scale dilation equations [25]. Since the GHM filter has two scaling and two wavelet functions, it has two lowpass subbands and two highpass subbands in the transform domain as mentioned in equation (3) - (4).

$$\begin{bmatrix} \emptyset_1(t) \\ \emptyset_2(t) \end{bmatrix} = \sqrt{2} \sum_k H_k \begin{bmatrix} \emptyset_1(2t-k) \\ \emptyset_2(2t-k) \end{bmatrix} \tag{3}$$

And
$$\begin{bmatrix} \Psi_1(t) \\ \Psi_2(t) \end{bmatrix} = \sqrt{2} \sum_k G_k \begin{bmatrix} \Psi_1(2t-k) \\ \Psi_2(2t-k) \end{bmatrix} \tag{4}$$

where

$$H_0 = \sqrt{2} \begin{bmatrix} \frac{3}{10} & \frac{2\sqrt{2}}{5} \\ -\frac{\sqrt{2}}{40} & -\frac{3}{20} \end{bmatrix} \qquad H_1 = \sqrt{2} \begin{bmatrix} \frac{3}{10} & 0 \\ \frac{9\sqrt{2}}{40} & \frac{1}{2} \end{bmatrix}$$

$$H_2 = \sqrt{2} \begin{bmatrix} 0 & 0 \\ \frac{9\sqrt{2}}{40} & \frac{-3}{20} \end{bmatrix} \qquad H_3 = \sqrt{2} \begin{bmatrix} 0 & 0 \\ \frac{-\sqrt{2}}{40} & 0 \end{bmatrix}$$

And

$$G_0 = \sqrt{2} \begin{bmatrix} \frac{-\sqrt{2}}{40} & \frac{-3}{20} \\ \frac{-1}{20} & \frac{-3\sqrt{2}}{20} \end{bmatrix} \qquad G_1 = \sqrt{2} \begin{bmatrix} \frac{9\sqrt{2}}{40} & \frac{-1}{2} \\ \frac{9}{20} & 0 \end{bmatrix}$$

$$G_2 = \sqrt{2} \begin{bmatrix} \frac{9\sqrt{2}}{40} & \frac{-3}{20} \\ \frac{-9}{20} & \frac{3\sqrt{2}}{20} \end{bmatrix} \qquad G_3 = \sqrt{2} \begin{bmatrix} \frac{-\sqrt{2}}{40} & 0 \\ \frac{1}{20} & 0 \end{bmatrix}$$

By examining the transform matrices of the scalar wavelet and multiwavelet as shown in Equations (3) and (4) respectively, it can be observed that in MWT domain there are first and second lowpass coefficients followed by first and second highpass filter coefficients rather than one lowpass coefficient followed by one highpass coefficient. Therefore, if we separate these four coefficients, there will be four subbands in the transform domain.

### III. FEATURES SELECTION

In feature-level image fusion, the selection of different features is an important task. The five different features used to characterize the information level contained in a specific portion of the image are Contrast Visibility, Spatial Frequency, Variance, Energy of Gradient (EOG), and Edge information. R.Maruthi and Dr.K.Sankarasubramanian proposed a fusion procedure by using a selection mode according to the magnitude of the spatial frequency and Visibility [26].

**Contrast Visibility***:* Contrast visibility calculates the deviation of a block of pixels from the block's mean value. Therefore it relates to the clearness level of the block. The visibility of the image block is obtained using equation (5).

$$VI = \frac{1}{p*q} \sum_{m,n \in B_k} \frac{|I(m,n)-\mu_k|}{\mu_k} \tag{5}$$

where $\mu_k$ and $p*q$ are the mean and size of the block $B_k$ respectively.

**Spatial Frequency***:* Spatial frequency measures the activity level in an image. It is used to calculate the frequency changes along rows and columns of the image. It is measured using equations (6) - (8).

$$SF = \sqrt{(RF)^2 + (CF)^2} \tag{6}$$

where

$$RF = \sqrt{\frac{1}{p*q}\sum_{m=1}^{p}\sum_{n=2}^{q}[I(m,n)-I(m,n-1)]^2} \tag{7}$$

$$CF = \sqrt{\frac{1}{p*q}\sum_{n=1}^{q}\sum_{m=2}^{p}[I(m,n)-I(m-1,n)]^2} \tag{8}$$

where I is the image and $p*q$ is the size of the image. A large value of spatial frequency describes the large information level in the image and therefore it measures the clearness of the image.

**Variance:** Variance measures the extent of focus in an image block. It is calculated using equation (9).

$$Variance = \frac{1}{p*q}\sum_{m=1}^{p}\sum_{n=1}^{q}(I(m,n)-\mu)^2 \tag{9}$$

where $\mu$ is the mean value of the block image and $p*q$ is the image size. A high value of variance shows the greater extent of focus in the image block.

4) **Energy of Gradient (EOG):** It is used to measure the amount of focus in an image. It is calculated using the equations (10) - (12).

$$EOF = \sum_{m=1}^{p-1}\sum_{n=1}^{q-1}(a_m^2 + a_n^2) \tag{10}$$

Where $\quad a_m = a(m+1,n) - a(m,n) \tag{11}$

and $\quad a_n = a(m,n+1) - a(m,n) \tag{12}$

where p and q represent the dimensions of the image block. A high value of energy of gradient shows greater amount of focus in the image block.
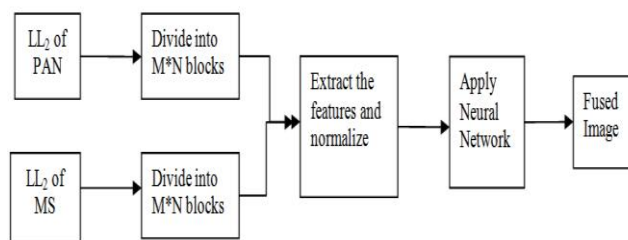


**Figure 2. Block diagram of the proposed method**

5) **Edge Information:** The Canny edge detector is used to identify the edge pixels in the image block. It returns 1 if the current pixel belongs to some edge in the image otherwise it returns 0. The edge feature is just the number of edge pixels contained within the image block.

#### A. Proposed BFMN Algorithm for Image Fusion

The block diagram of the proposed BFMN method is shown above in Figure 2. The proposed BFMN method uses multiwavelet transform as it has more number of scaling functions and wavelet functions. Each decomposition level of multiwavelet transform consists of 16 subbands. The proposed BFMN method also uses neural networks because the learning capability of neural networks makes it feasible to customize the image fusion process. The multiwavelet transform has the following advantages

1. shift variant
2. good directionality
3. basis offers a combination of orthogonality, symmetry, and compact support

The proposed BFMN method integrates multiwavelet transform with ANN because ANN based methods employ a nonlinear response function that iterates many times in a special network structure in order to learn the complex functional relationship between input and output training data. ANN based fusion method exploits the pattern recognition capabilities of ANN. Many of applications indicate that the

ANN-based fusion methods have more advantages than traditional statistical methods, especially when input multiple sensor data were incomplete or with much noise. The neural network will consists of three layers – input layer, hidden layer and output layer. The input layer has several neurons, which represent the feature factors extracted and normalized from the source images. The hidden layer has several neurons and the output layer can have one or more neurons.

The proposed BFMN algorithm is given below :

Algorithm : BFMN begin
Step.1   Read PAN and MS image.
Step.2   Apply second level decomposition to both the source images.
Step.3   Consider the Low-Low subcomponent of both the images. (let it be $LL_2$ sub component).
Step.4   Partition the $LL_2$ subcomponent of both the images into k blocks of M*N size and extract the features for every block. The features considered are contrast visibility, spatial frequency, energy of gradient, variance and edge information.
Step.5   Subtract the feature values of $j^{th}$ block of $LL_2$ subband of PAN image from the corresponding feature values of $j^{th}$ block of $LL_2$ subband of MS image. If the difference is 0 then denote it as 1 else -1.
Step.6   Construct an index vector for classification which will be given as an input for the Neural Network.
Step.7   Create a neural network with three layers and adequate number of neurons. Train the newly constructed neural network with random index value.
Step.8   Simulate the neural network with feature vector index value.
Step.9   If the simulated output > 1 then the $j^{th}$ subblock of $LL_2$ subband of PAN image is considered else the $j^{th}$ subblock of $LL_2$ subband of MS image is considered.
Step.10  Reconstruct the entire block and apply inverse transform to get back the fused image.
end

## IV.  QUALITY ASSESSMENT TECHNIQUES

To assess the quality of fused image, some quality measures are considered. These measures play an important role in various Image Processing applications. Goal of image quality assessment is to supply quality metrics that can predict perceived image quality automatically. While visual inspection has limitation due to human judgment, quantitative approach based on the evaluation of "distortion" in the resulting fused image is more desirable for mathematical modeling.

### A.  Quantitative Measures

The goals of the quantitative measures are normally used for the result of visual inspection due to the limitations of human eyes. In Mathematical modeling, quantitative measure is desirable. One can develop quantitative measure to predict perceived image quality. In this paper, the quality assessment is derived on BFMN method using noise-based measures to evaluate the noise of the fused image compared to the original MS image. Here the following optimal noise measures are implemented to judge the performance of fusion methods [19] as follows:

**Peak signal to noise ratio (PSNR):** PSNR is used to reveal the radiometric distortion of the fused image compared to the original image. It is defined using equation (13).

$$PSNR(dB) = 10\log_{10}\left(\frac{255*255}{MSE}\right) \quad (13)$$

where MSE is used to measure the spectral distortion in the fused image. It is defined using equation (14)

$$MSE = \frac{\sum_{i=1}^{M}\sum_{j=1}^{N}(I_R(i,j)-I_F(i,j)^2)}{M*N} \quad (14)$$

where $I_R(i,j)$ denotes pixel $(i,j)$ of the image reference and $I_F(i,j)$ denotes pixel $(i,j)$ of the fused image, $M*N$ is the image size.

**Mutual Information Measure (MIM):** MIM is used to furnish the      amount of information of the source image in the fused image. It is defined by using the equation (15).

$$I_{MN} = \sum_{x,y} P_{MN}(x,y)\log\frac{P_{MN}(x,y)}{P_M(x)P_N(y)} \quad (15)$$

where M, N are the two source images, $P_M(x)$ and $P_N(y)$ are the probability density functions of the individual images and $P_{MN}(x,y)$ is joint probability density function.

**Fusion Factor (FF) :** FF is used to measure the amount of information present in the fused image. It is defined by using the equation (16).

$$FF = I_{AF} + I_{BF} \quad (16)$$

where A and B are the two source images and F is the fused image. A higher value of FF indicates that fused image contains moderately good amount of information present in both the images.

**Standard Deviation (SD) :** SD is used to measure the level of contrast in the fused image. It is defined using equation (17).

$$SD = \sqrt{\sum_{i=0}^{L}(i - i')^2 h_F(i)} \quad (17)$$

where $i' = \sum_{i=0}^{L} ih_F$ and $h_F$ is the normalized histogram of fused image and L is the number of gray levels. A well contrast image has high standard deviation.

**Mean absolute error (MAE) :** MAE is used to measure the average magnitude of the errors in a set of forecasts, without considering their direction. It measures accuracy for continuous variables using equation (18).

$$MAE = \frac{1}{M*N}\sum_{x=0}^{M-1}\sum_{y=0}^{N-1}(I_R(x,y) - I_F(x,y)) \quad (18)$$

where $I_R(x,y)$ denotes pixel $(x,y)$ of the image reference and $I_F(x,y)$ denotes pixel $(x,y)$ of the fuse image and $M*N$ is the image size.

## V.  RESULT ANALYSIS

In this paper, two kinds of fusion methods are implemented and executed on PC with 2.4 G CPU and 2.0 G RAM using Matlab 7.6.0 to compare their fusion results. The experiment is conducted and tested on IRS-1C PAN and MS images for the locations Hyderabad, Vishakhapatnam, Mahaboobnagar, and Patancheru in India and on QuickBird and Landsat 7 image data.

This paper compares the present proposed BFMN method with previously proposed BFWN method [27] for fusing IRS-1D PAN and MS images about the locations Hyderabad, Vishakhapatnam, Mahaboobnagar, Patancheru, Landsat 7 and QuickBird images using the quality assessment metrics discussed in 4.1.
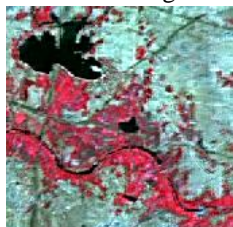
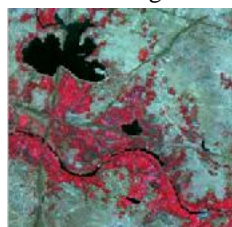The following are the fused images about the location Hyderabad by using the methods BFWN and BFMN.
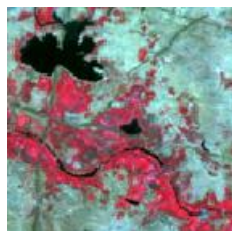
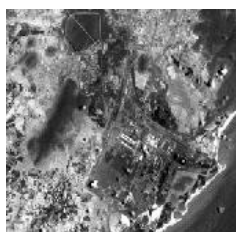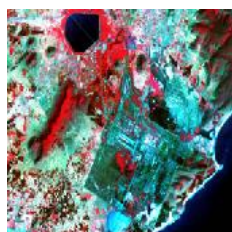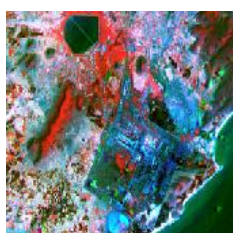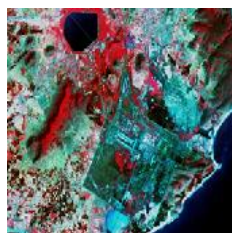PAN image      MS image

BFWN      BFMN

The following are the fused images about the location Vishakhapatnam by using the methods BFWN and BFMN.

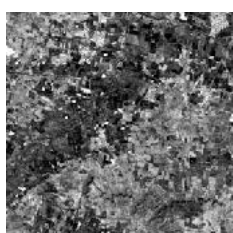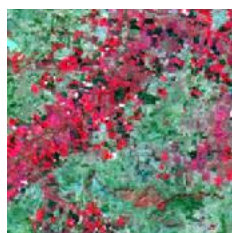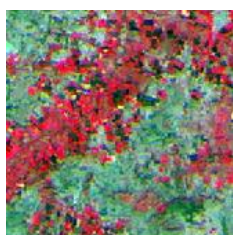PAN image      MS image

BFWN      BFMN

The following are the fused images about the location Mahaboobnagar by using the methods BFWN and BFMN.

PAN image      MS image
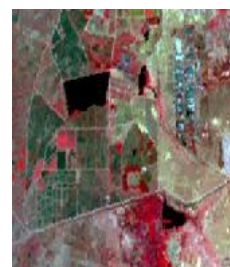
BFWN      BFMN

The following are the fused images about the location Patancheru by using the methods BFWN and BFMN.

PAN image      MS image

BFWN      BFMN

The following are the fusion results on Landsat 7 image data set by using the methods BFWN and BFMN.
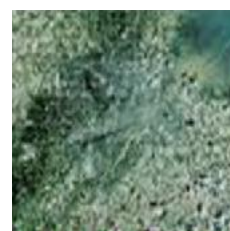
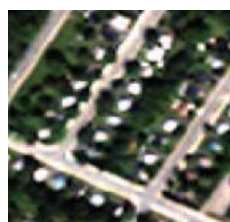PAN image      MS image

BFWN      BFMN

The following are the fusion results on QuickBird image data set by using the methods BFWN and BFMN.
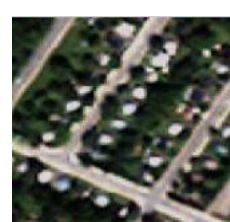
PAN image      MS image

BFWN      BFMN

The calculated values of PSNR, MIM, FS, SD and MAE for the methods BFWN and the proposed BFMN about the locations Hyderabad, Vishakhapatnam and Mahaboobnagar image data sets are mentioned in the Table I and about the locations Patancheru, Landsat 7 and QuickBird image data sets are mentioned in the Table II.

By comparing the values of PSNR of both the methods, the results show that the higher values of PSNR is achieved for the proposed BFMN method. It implies that high signal is preserved for the fused image. The graph is depicted in figure 3. Similarly, by comparing the values of SD of both the methods, the results show that the smaller values of SD is achieved for the proposed BFMN method. It indicates that not much deviation is induced in the fused image. The graph is depicted in figure 4.
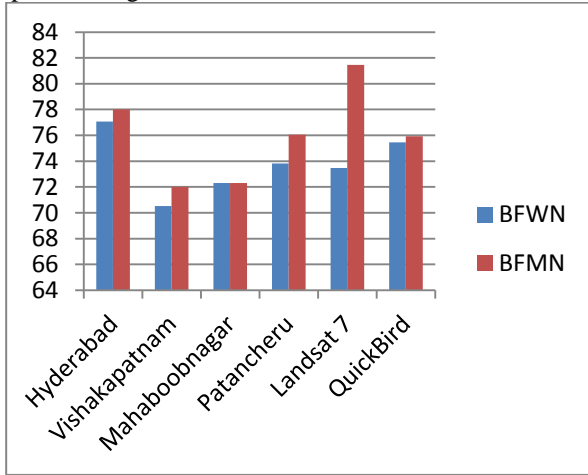


**Figure 3. Comparing PSNR values**

**Table I : Comparison of different metrics using BFWN and BFMN methods for Hyderabad image, Vishakhapatnam image and Mahaboobnagar image**

| Quality Metrics | Hyderabad Image | | Vishakhapatnam Image | | Mahaboobnagar Image | |
|---|---|---|---|---|---|---|
| | BFWN | BFMN | BFWN | BFMN | BFWN | BFMN |
| PSNR | 77.0658 | 78.0004 | 70.5083 | 72.0199 | 72.3011 | 72.3152 |
| MIM | 2.0289 | 2.4232 | 1.0235 | 1.4223 | 1.0060 | 1.0235 |
| FF | 4.0577 | 2.8463 | 2.0470 | 2.8446 | 2.0120 | 2.0471 |
| SD | 40.5197 | 35.7098 | 62.3872 | 55.1914 | 49.4440 | 44.2487 |
| MAE | 0.0161 | 0.0073 | 0.0357 | 0.0287 | 0.0291 | 0.0283 |

**Table II : Comparison of different metrics using BFWN and BFMN methods for Patancheru image, Landsat 7 image and QuickBird image**

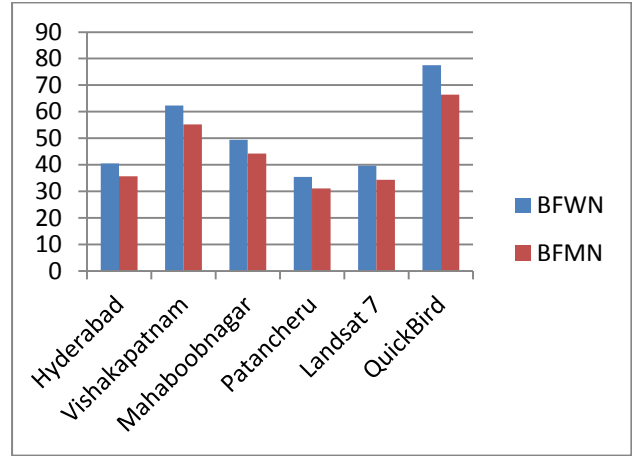| Quality Metrics | Patancheru Image | | Landsat 7 Image | | QuickBird Image | |
|---|---|---|---|---|---|---|
| | BFWN | BFMN | BFWN | BFMN | BFWN | BFMN |
| PSNR | 73.8269 | 76.0441 | 73.4789 | 81.4575 | 75.4508 | 75.9335 |
| MIM | 1.1985 | 1.5254 | 1.6842 | 1.1676 | 1.8487 | 1.8657 |
| FF | 2.3970 | 3.0507 | 3.3684 | 2.3352 | 3.6974 | 2.6114 |
| SD | 35.4804 | 31.1235 | 39.6275 | 34.4128 | 77.5713 | 66.4046 |
| MAE | 0.0258 | 0.0160 | 0.0296 | 0.0248 | 0.0194 | 0.0183 |



**Figure 4. Comparing SD values**

## VI.  CONCLUSION AND FUTURE WORK

The potentials of image fusion using the proposed BFMN method are explored. The various fusion results are analyzed by using quality performance metrics. For all the six image data sets, the higher value for PSNR is achieved for the proposed BFMN method. The higher value of PSNR implies that, the spectral information in MS image is preserved

effectively and high signal is preserved. The higher value of MIM is achieved for the proposed BFMN method for all five images except for the Landsat 7 image. The higher value of MIM indicates that

symmetry is achieved by retaining the spectral information. The higher value of FF is achieved for three pairs of images i.e., Vishakhapatnam, Mahaboobnagar and Patancheru images. The higher value of FF indicates that fused image contains moderately good amount of information present in both the images. For all the six image data sets, the smaller value for SD and MAE is obtained for the proposed BFMN method.  The smaller value of SD indicates that not much deviation is induced in the fused image and the smaller value of MAE indicates that the error rate is reduced in the fused image. The metric parameter PSNR and MIM are maximum for the proposed BFMN method, and SD and MAE are minimum for the proposed BFMN method. The metric parameter FF is equally maximum for the proposed BFMN method and BFWN. The experimental results indicate that BFMN outperforms the earlier BFWN method. Hence, it is ascertained that multiwavelet with NN method has superior performance than wavelet transform with NN method. The results are verified for LISS III images and the researches can extend their work in fusion for other types of images.

## REFERENCES

1. K. Kannan, S. Arumuga Perumal, K. Arulmozhi, "Performance Comparison of various levels of Fusion of Multi-focused Images using Wavelet Transform", 2010 International Journal of Computer Applications (0975 – 8887), Volume 1 – No. 6.
2. Jiang Dong, Dafang Zhuang, Yaohuan Huang and Jingying Fu, "Advances in Multi-sensor data fusion: algorithm and applications", Sensors 2009, 9, 7771, 7784; doi:10.3390/ s91007771.
3. Kai-Chieh Liang, Jin Li and C.-C. Jay Kuo, "Image Compression with Embedded Multiwavelet Coding".
4. Michael B. Martin and Amy E. Bell, "New Image Compression Techniques Using Multiwavelets and Multiwavelet Packets", IEEE TRANSACTIONS ON IMAGE PROCESSING, VOL. 10, NO. 4, APRIL 2001.
5. Fernando Pérez Nava and Antonio Falcón Martel, "Planar shape representation based on Multiwavelets".
6. Abdul Basit Siddiqui, M.Arfan Jaffar, Ayyaz Hussain, Anwar M. Mirza, "Block-based Feature-level Multi- focus Image Fusion", 5th International Conference on Future Information Technology (FutureTech), 2010 IEEE, 978-1-4244-6949-9/10.
7. G. Piella, "A region-based multiresolution image fusion algorithm", Information Fusion, 2002. Proceedings of Fifth International Conference on Information Fusion, 1557-1564.
8. "Effectiveness of Contourlet vs Wavelet Transform on Medical Image Compression: a Comparative Study", Negar Riazifar, and Mehran Yazdi, World Academy of Science, Engineering and Technology, 49, 2009.
9. Block feature based image fusion using multi wavelet transforms - Maziyar Khosravi, Mazaheri Amin - International Journal of Engineering Science and Technology (IJEST) - ISSN: 0975-5462 Vol. 3 No. 8 August 2011, 6644.
10. J. Lebrun and M. Vetterli, "Balanced multi wavelets and design," IEEE Trans. on Signal Processing, Vol. 46, No.4, pp. 1119-1124, Apr. 1998.
11. H. Wang, J. Peng, and W. Wu, "Fusion algorithm for multi sensor images based on discrete multi wavelet transform," IEE Proc. Vis. Image Signal Process., Vol. 149, No. 5, pp. 283-289, Oct. 2002.
12. Louis, E.K.; Yan, X.H. A neural network model for estimating sea surface chlorophyll and sediments from thematic mapper imagery. Remote Sens. Environ. 1998, 66, 153–165.
13. Dong. J.; Yang, X.; Clinton, N.; Wang, N. An artificial neural network model for estimating crop yields using remotely sensed information. Int. J. Remote Sens. 2004, 25, 1723–1732.
14. Hossein Sahoolizadeh, Davood Sarikhanimoghadam, and Hamid Dehghani, "Face Detection using Gabor Wavelets and Neural Networks", World Academy of Science, Engineering and Technology 45, 2008.
15. Shutao, L.; Kwok, J.T.; Yaonan W. Multifocus image fusion using artificial neural networks. Pattern Recognit. Lett.2002, 23, 985–997.
16. B.A.David and Y.David Solomon Raju, "Multi scale image fusion using GHM multi-wavelet", Global Journal of Advanced Engineering Technologies-Vol1, Issue1-2012.
17. S. Mallat, A Wavelet Tour of Signal Processing, Academic Press, Second Edition, 1998.
18. J. S. Geronimo, D. P. Hardin, and P. R. Massopust, Fractal functions and wavelet expansions based on several scaling functions," J. Approx. Theory, 1994.
19. G. Donovan, J. S. Geronimo, D. P. Hardin, and P. R. Massopust,\ Construction of orthogonal wavelets using fractal interpolation functions," preprint, 1994.
20. I Daubechies, Ten Lectures on Wavelets, pp. 251{254, SIAM, 1992.
21. T. Xia and Q. Jiang, "Optimal multifilter banks: Design, related symmetric extension transform and application to image compression," IEEE Trans. Signal Processing, vol. 47, pp. 1878–1889, July 1999.
22. S. S. Goh, Q. Jiang, and T. Xia, Construction of biorthogonal multiwavelets using the lifting scheme, preprint, 1998.
23. J. Y. Tham, L.-X. Shen, S. L. Lee, and H. H. Tan, "A general approach for analysis and application of discrete multiwavelet transforms," IEEE Trans. Signal Processing, vol. 48, pp. 457–464, Feb. 2000.
24. V. Strela and A. T.Walden, "Orthogonal and biorthogonal multiwavelets for signal denoising and image compression," Proc. SPIE, vol. 3391, pp. 96–107, 1998.
25. T. N. T. Goodman and S. L. Lee, "Wavelets of Multiplicity", Trans. Of the Amer. Math. Soc., Vol. 342, pp.307-324,1994.
26. Maziyar Khosravi and Mazaheri Amin, "Block Feature Based Image Fusion using Multi Wavelet Transforms", International Journal of Engineering Science and Technology (IJEST) Vol. 3 No. 8 August 2011.
27. C.M.Sheela Rani, V.VijayaKumar, B.Sujatha "An Efficient Block based Feature level image fusion technique using Wavelet transform and Neural network", "International Journal of Computer Applications", (0975-8887), Vol.52, No.12.